

CALL FOR PAPERS | *Metabolic Control by Inflammation and Immunity*

Myeloid cell TRAF3 promotes metabolic inflammation, insulin resistance, and hepatic steatosis in obesity

Zheng Chen,¹ Hong Shen,¹ Chengxin Sun,¹ Lei Yin,¹ Fei Tang,² Pan Zheng,² Yang Liu,² Robert Brink,⁴ and Liangyou Rui^{1,3}

¹Department of Molecular and Integrative Physiology, University of Michigan Medical School, Ann Arbor, Michigan;

²Department of Surgery, University of Michigan Medical School, Ann Arbor, Michigan; ³Department of Internal Medicine, University of Michigan Medical School, Ann Arbor, Michigan; and ⁴Garvan Institute of Medical Research, Darlinghurst, New South Wales, Australia

Submitted 10 October 2014; accepted in final form 18 January 2015

Chen Z, Shen H, Sun C, Yin L, Tang F, Zheng P, Liu Y, Brink R, Rui L. Myeloid cell TRAF3 promotes metabolic inflammation, insulin resistance, and hepatic steatosis in obesity. *Am J Physiol Endocrinol Metab* 308: E460–E469, 2015. First published January 27, 2015; doi:10.1152/ajpendo.00470.2014.—Myeloid cells, particularly macrophages, mediate metabolic inflammation, thus promoting insulin resistance and metabolic disease progression in obesity. Numerous cytokines, toxic metabolites, damage-associated molecular patterns, and pathogen-associated molecular patterns are involved in activating macrophages via their cognate receptors in obesity. TRAF3 (TNF receptor-associated factor 3) is a common signaling molecule for these ligands/receptors and negatively regulates the proinflammatory NF- κ B and MAPK pathways, but its metabolic activity is unknown. We here show that myeloid cell TRAF3 is required for metabolic inflammation and metabolic disease progression in obesity. Myeloid cell-specific deletion of *TRAF3* significantly attenuated insulin resistance, hyperglycemia, hyperinsulinemia, glucose intolerance, and hepatic steatosis in mice with either genetic (*ob/ob*) or high-fat diet (HFD)-induced obesity. Myeloid cell-specific deletion of *TRAF3* had the opposite effects on metabolic inflammation between obese and lean mice. It decreased the expression of proinflammatory cytokines in the liver and adipose tissue of obese mice and largely prevented HFD-induced inflammation in these metabolic tissues; by contrast, in lean mice, it increased the expression of proinflammatory cytokines in the liver and adipose tissue. These data suggest that, in obesity progression, myeloid TRAF3 functionally switches its activity from anti-inflammatory to proinflammatory modes, thereby coupling overnutrition to metabolic inflammation, insulin resistance, and metabolic disease.

metabolic inflammation; TRAF3; obesity; insulin resistance; steatosis

OBESITY IS ASSOCIATED WITH chronic, low-grade inflammation, which contributes to insulin resistance and metabolic disease (9, 14, 23, 29). Myeloid cells, particularly macrophages in adipose tissue and the liver, are believed to play a critical role in initiating and sustaining metabolic inflammation under obesity conditions (2, 10, 13, 17, 19). Adipocyte-derived lipolytic products, cytokines, and/or chemokines are involved in both recruiting monocytes and promoting macrophage M1 polarization, leading to adipose inflammation in obesity (2, 9, 11, 14, 23, 27). Additionally, damage-associated

molecular patterns (DAMPs) and pathogen-associated molecular patterns (PAMPs) also increase in obesity (2, 5, 9, 14, 23). The levels of endotoxins, particularly lipopolysaccharide (LPS) derived from gastrointestinal microbiota, are higher in obese subjects and animals (16). These proinflammatory metabolites, DAMPs and PAMPs, activate innate immune cells, particularly myeloid cells, through their cognate pattern recognition receptors (PRRs), including Toll-like receptors (TLRs), NOD-like receptors (NLRs), and RIG-I-like receptors (RLRs), thereby promoting obesity-associated chronic inflammation (2, 5, 9, 14, 23). However, the intracellular signaling pathways, which link these ligands and their receptors to insulin resistance and metabolic disease, are not fully understood.

TNF receptor-associated factor 3 (TRAF3) is a TRAF family member with a molecular mass of ~62 kDa. *TRAF3* knockout mice die shortly after birth (28), indicating that TRAF3 has a unique, essential function and cannot be replaced by other TRAF family members. TRAF3 is a ubiquitously expressed cytoplasmic adaptor protein and is involved in mediating cytokine receptor, TLR, PKR, NLR, and RLR signaling in myeloid cells (6, 7, 18, 21, 24, 26). TRAF3 inhibits NF- κ B-inducing kinase (NIK) by promoting ubiquitination and degradation of NIK (12). A subset of cytokines stimulates ubiquitination and degradation of TRAF3, thus activating NIK and the noncanonical NF- κ B2 pathway (24). TRAF3 inhibits activation of the canonical NF- κ B1 pathway through competing with TRAF2 and/or TRAF6 for the common binding sites in cytokine receptors and/or upstream adaptors (1, 8, 30, 31). TRAF3 negatively regulates activation of the MAPK pathway in response to interleukin (IL)-1, LPS, and CD40L, and TRAF3 degradation is required for these ligands to activate the MAPK pathway (15, 25). In addition to inhibiting the proinflammatory NF- κ B and MAPK pathways, TRAF3 also binds to and activates TBK1 and IKKi and mediates TLR, RLR, and PKR stimulation of the IRF3/IRF7 pathways (6, 7, 18). The TBK1/IKKi/IRF3/IRF7 pathways mediate PAMP- and DAMP-stimulated expression and secretion of type I interferons and IL-10 (6, 7, 18). Therefore, TRAF3 in myeloid cells acts as an anti-inflammatory protein to inhibit proinflammatory NF- κ B and MAPK pathways and to increase the expression of anti-inflammatory IL-10. Indeed, deletion of *TRAF3* increases the expression and secretion of proinflammatory TNF α , IL-1,

Address for reprint requests and other correspondence: L. Rui, Dept. of Molecular & Integrative Physiology, Univ. of Michigan Medical School, Ann Arbor, MI 48109 (e-mail: ruiy@umich.edu).

IL-6, and IL-12 in cultured myeloid cells (6, 18). However, the function of TRAF3 in the setting of obesity has not been examined.

In this study, we examined the inflammatory and metabolic functions of TRAF3 in myeloid cells by using myeloid cell-specific TRAF3 knockout (MKO) mice. We confirmed that myeloid TRAF3 has anti-inflammatory properties in lean mice. TRAF3 appears to gain proinflammatory activity during the course of obesity progression. Accordingly, myeloid cell-specific deletion of TRAF3 markedly improves insulin resistance, glucose intolerance, and hepatic steatosis in MKO mice with either dietary or genetic obesity. Our data suggest that obesity-associated factors promote an anti-inflammation to pro-inflammation switch of TRAF3 functional modes. This mode switch of TRAF3 activity may contribute to metabolic inflammation, insulin resistance, and metabolic disease progression in obesity.

MATERIALS AND METHODS

Animals. Animal experiments were conducted following protocols approved by the University Committee on the Use and Care of Animals (UCUCA). TRAF3^{lox/lox} mice were provided by Dr. Robert Brink (Garvan Institute of Medical Research, Australia). LysM-Cre mice were from the Jackson Laboratory (Bar Harbor, ME). MKO mice were generated by crossing TRAF3^{lox/lox} mice with LysM-Cre mice (in C57Bl/6 genetic background). Mice were housed on a 12:12-h light-dark cycle in the Unit for Laboratory Animal Medicine at the University of Michigan and fed ad libitum either a normal chow diet (9% fat; TestDiet, St. Louis, MO) or a HFD (60% fat; Research Diets, New Brunswick, NJ).

Glucose, insulin, pyruvate, lactate, and glucagon tolerance tests. Blood samples were collected from tail veins. Plasma insulin was measured using Rat Insulin RIA kits (Millipore (Millipore-RI-13K)). For glucose (GTT), insulin (ITT), pyruvate (PTT), or lactate (LTT) tolerance tests, mice were fasted for 16 h and intraperitoneally injected with glucose (2 g/kg body wt for mice fed normal chow or a HFD; 0.5 g/kg for DKO and ob/ob;TRAF3^{lox/lox} mice), lactate (0.5 g/kg for DKO and ob/ob;TRAF3^{lox/lox} mice), or pyruvate (1 g/kg for

HFD-fed mice), and blood glucose was measured 0, 15, 30, 60, and 120 min after injection. For ITT and glucagon tolerance tests, mice were fasted for 6 h and intraperitoneally injected with insulin (0.75 U/kg body wt for mice fed a normal chow diet, 1 U/kg for HFD-fed mice, 4 U/kg for DKO and ob/ob;TRAF3^{lox/lox} mice) or glucagon (Sigma G2044) (10 µg/kg for HFD-fed mice, and 6 µg/kg for DKO and ob/ob;TRAF3^{lox/lox} mice), and blood glucose was measured 0, 15, 30, 60, and 120 min after injection.

Fluorescence-activated cell sorting (FACS) analysis. Epididymal fat pads were isolated, minced in Hanks' balanced salt solution (HBSS, Invitrogen) containing 0.5% BSA, and digested with 1 mg/ml collagenase type I (Worthington, Lakewood, NJ) at 37°C for 20–30 min. Cell suspension was filtered through a 100-µm filter and subjected to centrifugation at 500 g for 10 min. Stromal vascular fractions (SVFs) in cell pellets were washed with PBS and resuspended in HBSS supplemented with 2% FBS. SVFs were stained with the indicated antibodies in HBSS containing 2% FBS at 4°C for 20 min and subsequently subjected to FACS analyses using an LSR II flow cytometer (BD Biosciences, San Jose, CA). Data were analyzed with FlowJo software (Tree Star, Ashland, OR). Flow antibodies were as follows: PE-Cy7-conjugated anti-mouse CD45.2 (clone 104, eBioscience), PerCP-Cy5.5-conjugated anti-mouse F4/80 (clone BM8, BioLegend), PE-conjugated anti-mouse CD11c (clone N418, eBioscience), and APC-conjugated anti-mouse CD301 (AbD Serotec).

Immunoblotting. Mice were fasted for 20–24 h and administered insulin (2 U/kg body wt for HFD-fed mice, 4 U/kg for DKO and ob/ob;TRAF3^{lox/lox} mice) via the inferior vena. Tissues were isolated 5 min after injection and homogenized in a lysis buffer (50 mM Tris-HCl, pH 7.5, 1.0% NP-40, 150 mM NaCl, 2 mM EGTA, 1 mM Na₃VO₄, 100 mM NaF, 10 mM Na₄P₂O₇, 1 mM PMSF, 10 µg/ml aprotinin, 10 µg/ml leupeptin). Tissue extracts were immunoblotted with antibodies against phospho-Akt (pSer⁴⁷³, Cell Signaling, no. 4060; pThr³⁰⁸, Santa Cruz Biotechnology, sc-16646-R), or Akt (Cell Signaling, no. 4691). Phosphorylation was quantified using Odyssey software and normalized to total Akt levels.

Immunostaining. Frozen liver sections (7 µm) were immunostained with anti-F4/80 antibody (eBioscience, San Diego, CA, 14-4801-82, 1:500). Liver or white adipose tissue paraffin sections (5 µm) were stained with hematoxylin and eosin (H&E).

Table 1. Primer sequences for qPCR

Genes	Forward	Reverse
36B4	5'-AAGGCGCTCCTGGCATTGTCT-3'	5'-CCGCAGGGGAGCAGTGGT-3'
ApoB	5'-CCAGAGTGTGGAGCTGAATGT-3'	5'-TTGCTTTTATAGGAGCCTAGC-3'
Arg1	5'-TCCAAGCCAAAGTCCTTAGAG-3'	5'-GGAGCTGTCAATTAGGGACATC-3'
CD36	5'-GGAGTGGTGATGTTTGTGCT-3'	5'-GCACACACCACCATTTCTCT-3'
ChREBP	5'-CTGGGGACCTAAACAGGAGC-3'	5'-GAAGCCACCTATAGCTCCC-3'
CPT1	5'-CTGATGACGGCTATGGTGT-3'	5'-GTGAGGCCAAACAAGGTGATA-3'
DGAT1	5'-CGTGGTATCCTGAATTGGTG-3'	5'-GGCGTCTCAATCTGAAAT-3'
F4/80	5'-CTTTGGCTATGGGCTTCCAGTC-3'	5'-GCAAGGAGGACAGAGTTTATCGTG-3'
FAS	5'-CTCGGAGTTTAAAGCTGAGG-3'	5'-TGTACTCCTCCCTCTGTGG-3'
G6Pase	5'-CCGGTGTGTTGAACGTCATCT-3'	5'-CAATGCCTGACAAGACTCCA-3'
IL-10	5'-CTGGACAACATACTGCTAACCG-3'	5'-GGGCATCACTTCTACCAGGTAA-3'
IL-1Ra	5'-GCTCATTGCTGGGTACTTACAA-3'	5'-CCAGACTTGGCACAAAGACAGG-3'
IL-1β	5'-GCCTTGGGCCTCAAAGGAAAGAATC-3'	5'-GGAAGACACAGATTCATGGTGAAG-3'
IL-6	5'-AGCCAGAGTCCTTCAGA-3'	5'-GGTCCTTAGCCACTCCT-3'
MCAD	5'-ACCTGTGGAGAAGCTGATG-3'	5'-AGCAACAGTGCTTGGAGCTT-3'
mGPAT1	5'-ACCGTGAGAGTGCCACATACT-3'	5'-GAGAGATCGCTACAGCACAC-3'
MTP	5'-CTCCACAGTGCAGTTCTCACA-3'	5'-AGAGACATATCCCTGCCTGT-3'
PEPCK	5'-ATCATCTTTGGTGGCCGTAG-3'	5'-ATCTTGCCTTGTGTTCT-3'
PPARγ	5'-CCAGAGTCTGCTGATCTGGC-3'	5'-GCCACCTCTTTGCTCTGATC-3'
SCD1	5'-AGGTGCCTTTAGCCACTGA-3'	5'-CCAGAGTTTCTTGGGTTGA-3'
SREBP1	5'-AACGTCACTTCCAGCTAGAC-3'	5'-CCACTAAGGTGCCTACAGAGC-3'
TNFα	5'-CATCTTCTCAAATTCGAGTGACAA-3'	5'-TGGGAGTAGACAAGGTACAAACC-3'
Ym1	5'-CACCATGGCCAAGCTCATTCTGT-3'	5'-TATTGGCCTGCTTAGCCCAACT-3'

Quantitative real-time PCR. Total RNAs were extracted using TRIzol reagent (Invitrogen Life Technologies, Carlsbad, CA). The first-strand cDNAs were synthesized using random primers and M-MLV reverse transcriptase (Promega, Madison, WI). qPCR was performed using Absolute QPCR SYBR Mix (Thermo Fisher Sci-

tific, UK) and Mx3000P real-time PCR system (Stratagene, LA Jolla, CA). qPCR primers are listed in Table 1.

Bone marrow-derived macrophages and hepatocyte glucose production assays. Primary bone marrow cells were isolated from *TRAF3^{flox/flox}* and MKO male mice (7–10 wk) and differentiated into

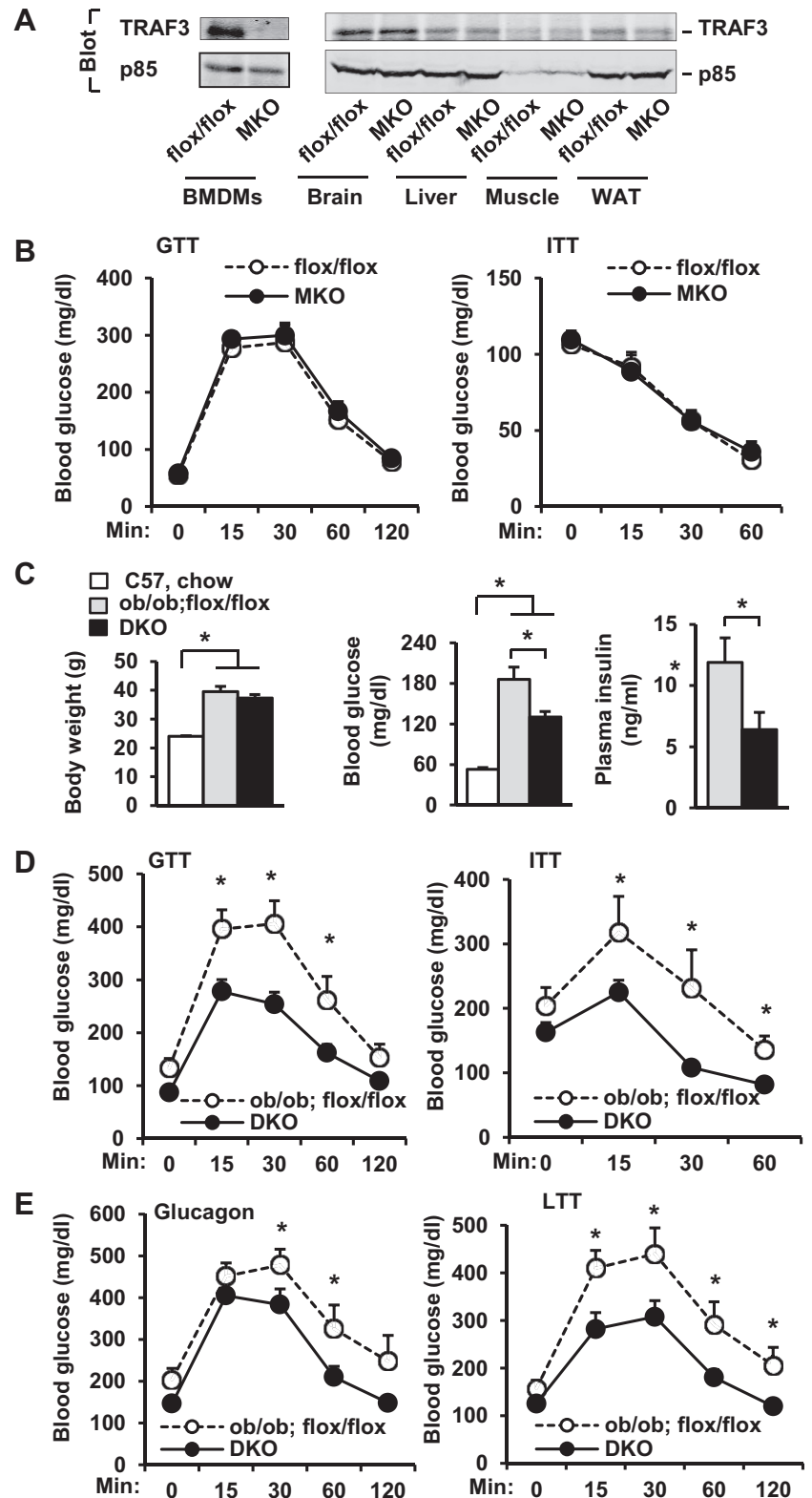


Fig. 1. Deletion of myeloid *TRAF3* (TNF receptor-associated factor 3) protects against insulin resistance and type 2 diabetes in *ob/ob* mice. BMDMs, bone marrow-derived macrophages; MKO, myeloid cell-specific *TRAF3* knockout; DKO, myeloid cell-specific *TRAF3* knockout in *ob/ob* mice. **A**: cell or tissue extracts were immunoprecipitated (IP) and immunoblotted with anti-*TRAF3* antibody. Extracts were also immunoblotted with anti-p85 antibody. **B**: GTT (2 g/kg body wt) and ITT (0.75 U/kg body wt) were measured in male mice at 18–20 wk of age. In each group, $n = 6-7$. **C–E**: experiments were performed in male mice at 8–10 wk of age. **C**: body weight and fasting (~16 h) blood glucose and plasma insulin: C57BL/6 males fed a normal chow diet, $n = 8$; *ob/ob;flox/flox*, $n = 5-10$; DKO, $n = 7-13$. **D**: GTT (0.5 g/kg body wt) and ITT (4 U/kg body wt): *ob/ob;flox/flox*, $n = 8-9$; DKO, $n = 13$. **E**: glucagon tolerance tests (6 μ g/kg body wt) and lactate tolerance tests (0.5 g/kg body wt): *ob/ob;flox/flox*, $n = 9$; DKO, $n = 11-12$. Values are presented as means \pm SE. * $P < 0.05$.

bone marrow-derived macrophages (BMDMs) as described previously (22). BMDMs were treated without or with LPS (20 ng/ml) for 4 h and washed extensively with PBS and cultured in fresh growth medium. Conditioned medium was collected 20 h later. Primary hepatocytes were isolated from wild-type male mice (7–10 wk) and subjected to glucose production assays in the presence or absence of 100 nM dexamethasone (Dex) and 10 μ M *N*⁶,2'-*O*-dibutyryl adenosine 3',5'-cyclic monophosphate sodium salt (DB-cAMP) as described previously (4). Primary hepatocytes were pretreated with conditioned medium for 4 h prior to glucose production assays.

Statistical analysis. Data are presented as means \pm SE. Differences between groups were analyzed by two-tailed Student's *t*-tests. *P* < 0.05 was considered statistically significant.

RESULTS

Myeloid cell-specific deletion of TRAF3 improves insulin resistance and glucose intolerance in leptin-deficient ob/ob mice. To generate MKO mice, *TRAF3*^{flox/flox} mice, which were generated and verified previously (21), were crossed with

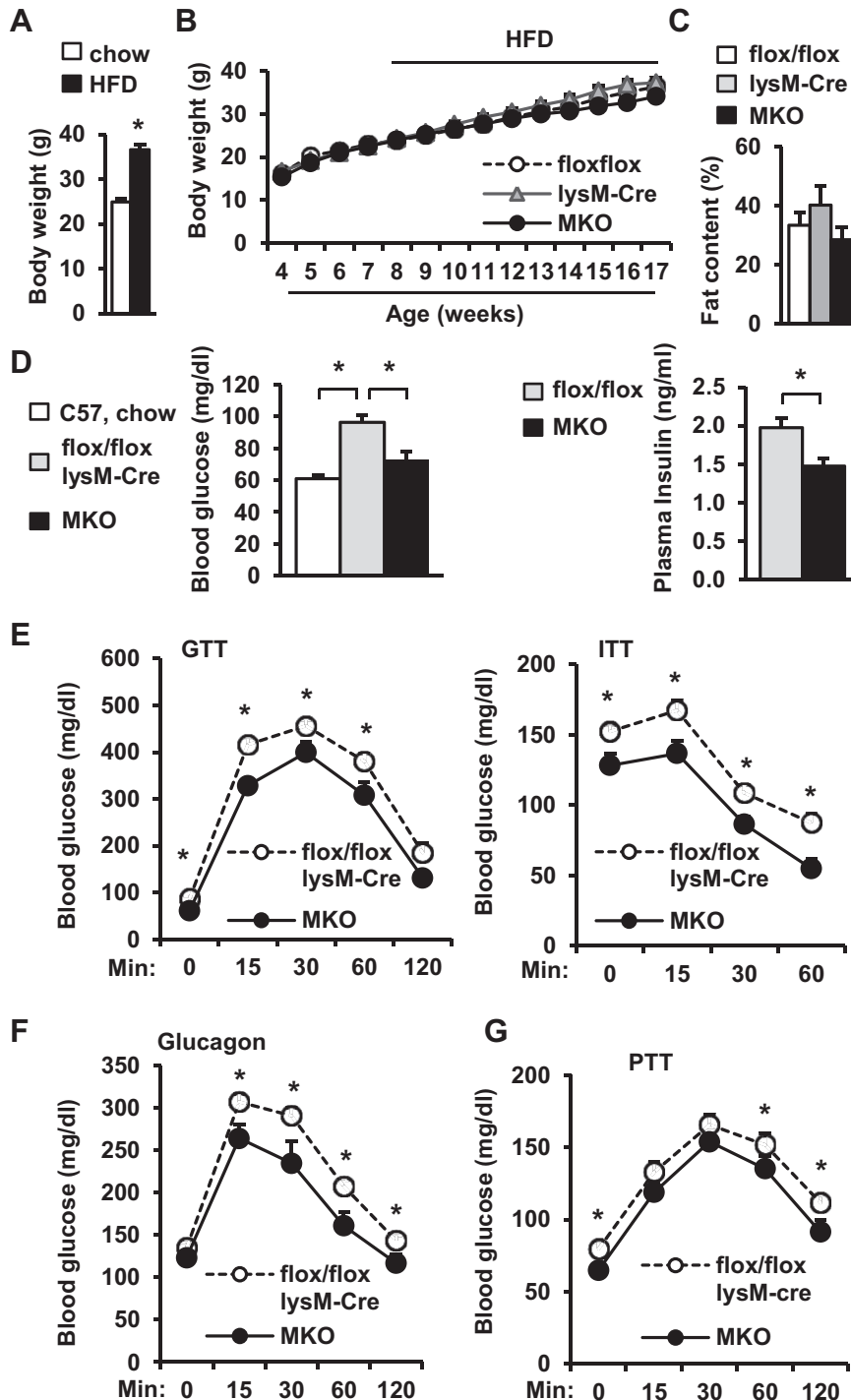


Fig. 2. Deletion of myeloid *TRAF3* attenuates high-fat diet (HFD)-induced insulin resistance and glucose intolerance. *A:* Body weight. C57BL/6 males (7–8 wk) fed a normal chow diet or a HFD for 10–12 wk: Chow, *n* = 7; HFD, *n* = 14. *B* and *C:* *TRAF3*^{flox/flox}, *lysM-Cre* and MKO male mice (7–8 wk) were fed a HFD for 10–12 wk. *B:* growth curves: *TRAF3*^{flox/flox}, *n* = 15; *lysM-Cre*, *n* = 12; MKO, *n* = 11. *C:* fat content: *TRAF3*^{flox/flox}, *n* = 14; *lysM-Cre*, *n* = 5; MKO, *n* = 12. *C–F:* male mice (7–8 wk) were fed a HFD, and experiments were performed 10–12 wk later. A combination of *TRAF3*^{flox/flox} mice and *lysM-Cre* mice (control): *n* = 20–25; MKO, *n* = 9–15. *D:* fasting (~16 h) blood glucose and plasma insulin. *E:* GTT (2 g/kg body wt) and ITT (1 U/kg body wt insulin). *F:* glucagon tolerance tests (10 μ g/kg body wt). *G:* PTT (pyruvate: 1 g/kg body wt). Values are presented as means \pm SE. * *P* < 0.05.

lysozyme M-Cre (*lysM-Cre*) transgenic mice. TRAF3 protein was detected in macrophages derived from *TRAF3^{flox/flox}* but not MKO mice (Fig. 1A). TRAF3 expression was normal in the brain, liver, skeletal muscle, and epididymal white adipose tissue (WAT) of MKO mice (Fig. 1A). MKO mice, fed a normal chow diet, had relatively normal body weight and blood glucose levels (data not shown). Insulin sensitivity and glucose tolerance, as estimated by ITT and GTT, were similar between MKO and *TRAF3^{flox/flox}* mice (Fig. 1B). GTT and ITT are likely to be similar between *TRAF3^{flox/flox}* and wild-type mice.

To determine whether myeloid TRAF3 contributes to insulin resistance in obesity, we deleted *TRAF3* specifically in myeloid cells of leptin-deficient *ob/ob* mice (designated DKO mice; genotype *ob/ob;TRAF3^{flox/flox};lysM-Cre*) by a series of crossing of MKO mice with *ob/+* mice. Body weight was similar between *ob/ob;TRAF3^{flox/flox}* (control) and DKO male mice, but both *ob/ob;TRAF3^{flox/flox}* and DKO mice were significantly heavier than wild-type C57BL/6 male mice fed a normal chow diet (Fig. 1C). Deletion of myeloid *TRAF3* significantly attenuated hyperglycemia and hyperinsulinemia in DKO mice relative to those in *ob/ob;TRAF3^{flox/flox}* mice, although blood glucose levels were still higher in both DKO and *ob/ob;TRAF3^{flox/flox}* mice than in lean C57BL/6 mice (Fig. 1C). DKO mice had significantly improved glucose tolerance and insulin sensitivity (Fig. 1D). We previously reported that hepatocyte-specific deletion of *TRAF2* results in glucagon resistance (3). Similarly, myeloid cell-specific deletion of *TRAF3* also decreased the ability of glucagon to increase blood glucose levels in DKO mice (Fig. 1E, left). Hepatic gluconeogenesis, estimated by LTT, was also lower in DKO mice (Fig. 1E, right). We performed PTT in DKO mice, but mice died after pyruvate injection. Together, these data suggest that myeloid cell TRAF3 promotes systemic insulin resistance, hyperglycemia, and glucose intolerance in *ob/ob* mice.

Myeloid cell-specific deletion of TRAF3 ameliorates insulin resistance and glucose intolerance in mice with dietary obesity. To verify diet-induced obesity, we monitored the body weights of C57BL/6 male mice fed a normal chow diet or a HFD. HFD-fed mice developed the obesity phenotypes as expected (Fig. 2A). To determine whether myeloid cell TRAF3 is involved in diet-induced insulin resistance and metabolic disease, MKO mice were fed a HFD. Body weight and fat content were similar between MKO, *TRAF3^{flox/flox}*, and *lysM-Cre* mice (Fig. 2, B and C). Blood glucose, glucose tolerance, and insulin tolerance were similar between *TRAF3^{flox/flox}* and *lysM-Cre* mice (data not shown), so a combination of these two genotypes was used as a control. Overnight fasting blood glucose levels were significantly lower in MKO mice than in *TRAF3^{flox/flox}* and *lysM-Cre* mice (Fig. 2D). Fasting blood glucose was slightly higher in HFD-fed MKO mice than in lean C57BL/6 males fed a normal chow diet, but the difference was not statistically significant ($P = 0.1$; Fig. 2D). Overnight fasting plasma insulin levels were also lower in MKO than in *TRAF3^{flox/flox}* mice (Fig. 2D). MKO mice had significantly improved insulin sensitivity and glucose tolerance relative to control mice (Fig. 2E) and displayed glucagon resistance (Fig. 2F). Hepatic gluconeogenesis, as measured by PTT, was also lower in MKO mice than in *TRAF3^{flox/flox}* mice (Fig. 2G). These observations indicate that TRAF3 in myeloid cells contributes to diet-induced insulin resistance and type 2 diabetes progression.

Myeloid cell-specific deletion of TRAF3 attenuates hepatic steatosis in obese mice. Obesity is associated with nonalcoholic fatty liver disease (NAFLD). To determine whether myeloid TRAF3 is involved in NAFLD progression, we measured liver lipid content in TRAF3-deficient mice with either genetic or dietary obesity. Both liver weight and triacylglycerol (TAG) content were significantly lower in DKO mice than in *ob/ob;TRAF3^{flox/flox}* control mice (Fig. 3A). Liver weight and TAG content were also lower in MKO mice than in *TRAF3^{flox/flox}* or *lysM-Cre* mice fed a HFD (Fig. 3B). Liver lipid droplet numbers

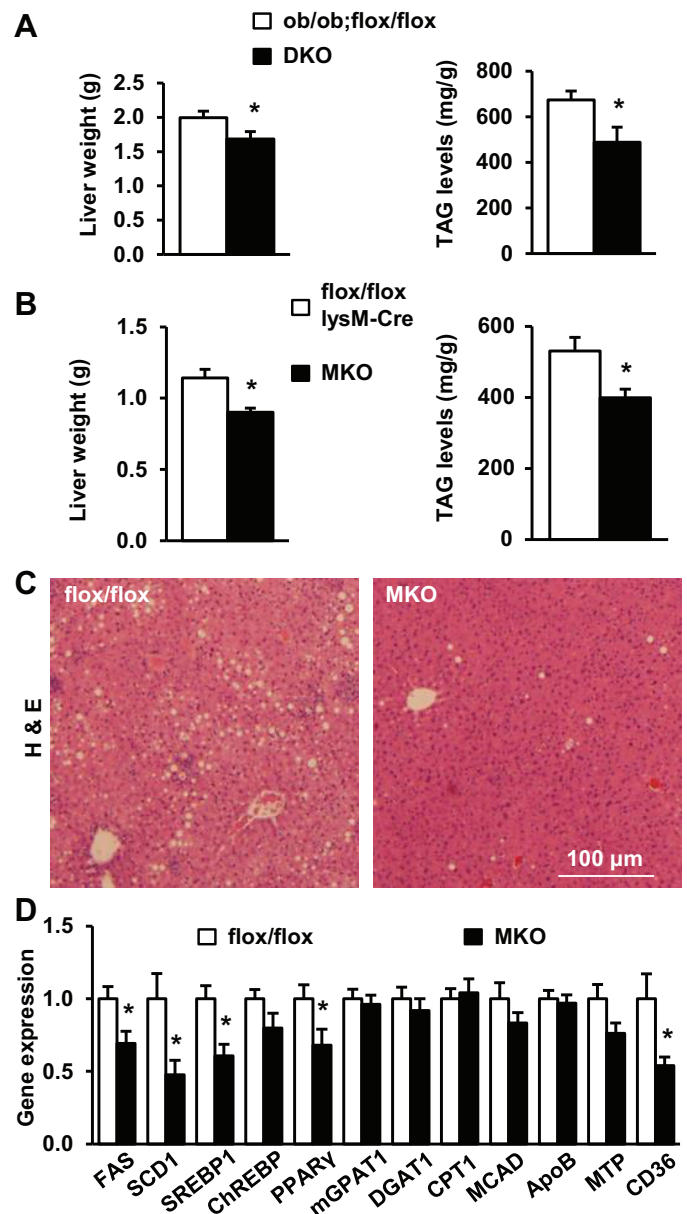


Fig. 3. Deletion of myeloid *TRAF3* attenuates hepatic steatosis in obesity. A: liver weight and triacylglycerol (TAG) levels (normalized to liver weight) in male mice at 10–12 wk of age. *ob/ob;flox/flox*, $n = 10$; DKO, $n = 5$ –10. B–D: male mice (7–8 wk) were fed a HFD for 10–12 wk. B: liver weight and TAG levels (normalized to liver weight). Combination of *TRAF3^{flox/flox}* mice and *lysM-Cre* mice (control), $n = 23$ –24; MKO, $n = 10$ –12. C: representative H&E staining of liver sections. D: gene expression in the liver was measured by qPCR and normalized to 36B4 expression. *TRAF3^{flox/flox}*, $n = 11$ –12; MKO, $n = 10$ –12. Values are presented as means \pm SE. * $P < 0.05$.

were lower in MKO mice than in *TRAF3^{lox/flox}* mice (Fig. 3C). The expressions of hepatic lipogenic genes (e.g., *FAS*, *SCD1*, *SREBP1*, and *PPAR γ*) were lower in MKO mice (Fig. 3D). These observations indicate that TRAF3 in myeloid cells promotes hepatic lipogenesis in obesity, contributing to NAFLD development.

Myeloid cell-specific deletion of TRAF3 improves insulin signal transduction in obese mice. To further study the role of myeloid TRAF3 in regulating insulin sensitivity, we examined insulin signaling in TRAF3-deficient mice by measuring phosphorylation of Akt, a key downstream insulin signaling molecule. Insulin stimulated phosphorylation of Akt (pThr³⁰⁸ and pSer⁴⁷³) in the liver, skeletal muscle, and adipose tissue of *ob/ob* mice and myeloid cell-specific deletion of *TRAF3* increased insulin-stimulated phosphorylation of Akt in these

tissues of DKO mice (Fig. 4A). Similarly, insulin-stimulated phosphorylation of Akt (pThr³⁰⁸) in the liver and muscle was also higher in MKO than in *TRAF3^{lox/flox}* mice fed a HFD (Fig. 4B). Akt phosphorylation was quantified and normalized to total Akt levels. Insulin-stimulated Akt phosphorylation was further normalized to basal levels of Akt phosphorylation in order to calculate fold induction. Insulin-stimulated phosphorylation of Akt at both pThr³⁰⁸ and pSer⁴⁷³ was significantly higher in DKO than in *ob/ob;TRAF3^{lox/flox}* mice (Fig. 4A, right). Insulin-stimulated phosphorylation of pThr³⁰⁸ and pSer⁴⁷³ was also higher in MKO than in *TRAF3^{lox/flox}* mice fed a HFD (Fig. 4B, right). These data suggest that myeloid TRAF3 contributes to suppression of insulin signaling in metabolic tissues of obese mice.

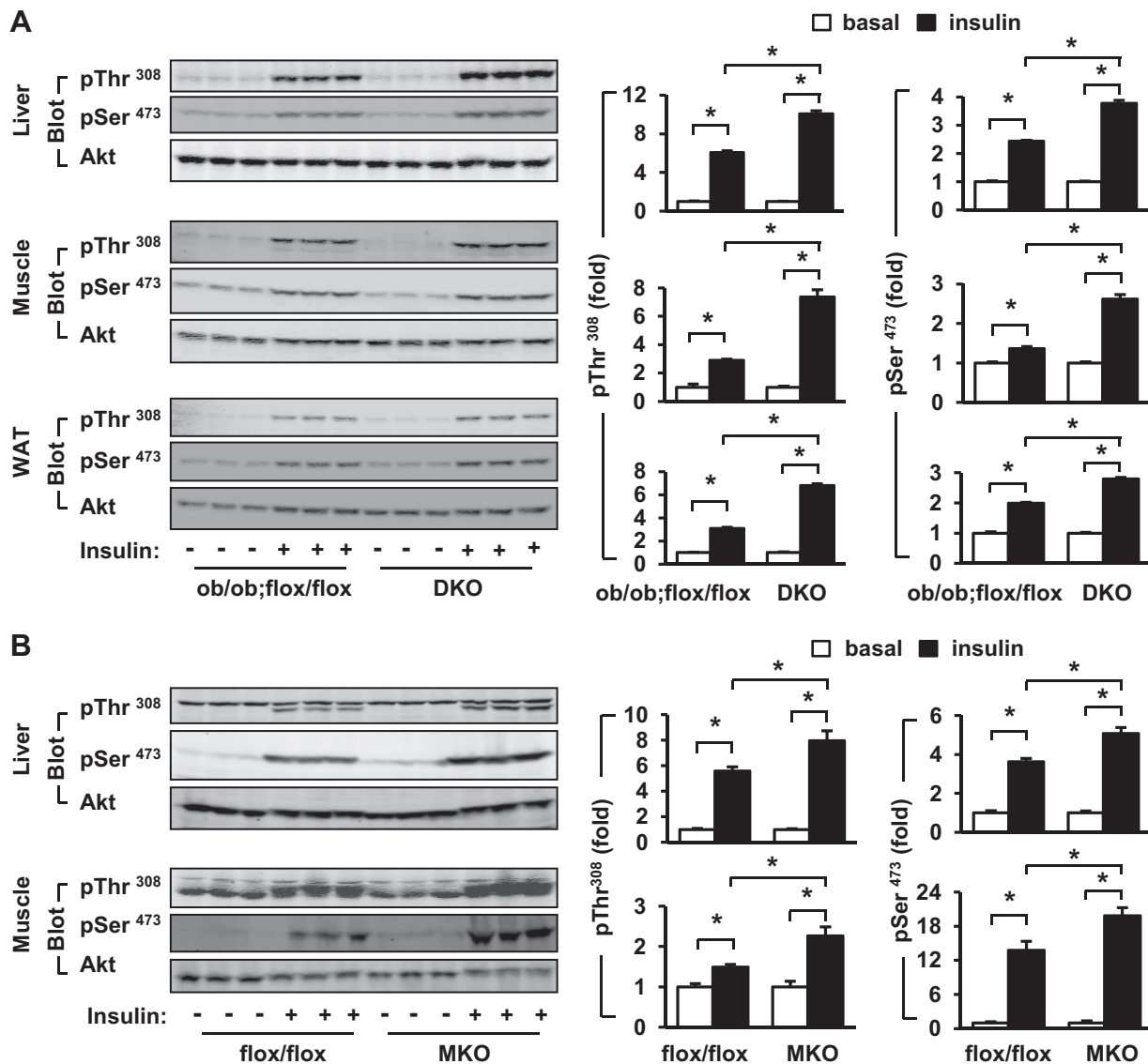


Fig. 4. Deletion of myeloid *TRAF3* improves insulin signaling in mice with obesity. **A**: male mice (10–12 wk) were fasted for 20–24 h and injected with insulin (4 U/kg body wt) via inferior vena. Tissue extracts were prepared 5 min after injection and immunoblotted with antibodies against phospho-Akt (pSer⁴⁷³ or pThr³⁰⁸) or Akt. Phosphorylation was quantified and normalized to total Akt levels. Insulin-stimulated Akt phosphorylation in *ob/ob; flox/flox* or DKO mice was further normalized to basal phosphorylation of Akt in *ob/ob; flox/flox* or DKO mice, respectively, and data were presented as fold induction. *ob/ob; flox/flox*, *n* = 3; DKO, *n* = 3. **B**: male mice (7–8 wk) were fed a HFD for 10–12 wk. Mice were fasted for 20–24 h and injected with insulin (2 U/kg body wt). Tissue extracts were prepared 5 min after injection and immunoblotted with indicated antibodies. Akt phosphorylation was quantified and presented as described in **A**. *TRAF3^{lox/flox}*, *n* = 3; MKO, *n* = 3. Values are presented as means ± SE. **P* < 0.05.

Glucose production rates are lower in primary hepatocytes pretreated with TRAF3-deficient macrophage-conditioned medium. Hepatic gluconeogenesis plays an important role in diabetes progression (20). We proposed that myeloid TRAF3 might regulate hepatocyte glucose production in a paracrine fashion. To test this idea, we examined the effect of TRAF3-deficient macrophage-conditioned medium on the glucose production capability of primary hepatocytes. BMDMs were prepared from MKO and *TRAF3^{flox/flox}* (control) mice and activated by pretreatment with LPS for 4 h. LPS-containing medium was replaced with fresh medium, and macrophage-conditioned medium was collected 20 h later. Primary hepatocytes, which were isolated from normal mice, were pretreated with conditioned medium and subjected to glucose production assays in the absence (basal) or presence of Dex and DB-cAMP stimulation. Dex and DB-cAMP were commonly used to mimic counterregulatory hormone stimulation (4). Dex/DB-cAMP increased glucose production rates as expected (Fig. 5A). For conditioned medium collected from unstimulated BMDMs, both basal and Dex/DB-cAMP-stimulated glucose production rates were similar between MKO and *TRAF3^{flox/flox}* groups (Fig. 5A). These data suggest that myeloid TRAF3 is not involved in the regulation of hepatic gluconeogenesis by quiescent macrophages. In contrast, for conditioned medium collected from LPS-stimulated BMDMs, Dex/DB-cAMP-stimulated glucose production rates were significantly lower in the MKO group than in the *TRAF3^{flox/flox}* group (Fig. 5B). The expressions of *G6Pase* and *PEPCK*, two key gluconeogenic genes, were also lower in the MKO group than in the *TRAF3^{flox/flox}* group (Fig. 5C). These data suggest that upon macrophage activation myeloid TRAF3 is able to increase hepatocyte gluconeogenesis in a paracrine manner.

HFD- and obesity-associated factors promote an anti-inflammation to pro-inflammation switch of TRAF3 activity modes. TRAF3 was reported to negatively regulate proinflammatory NF- κ B and MAPK pathways in myeloid cells and suppress the expression and secretion of proinflammatory cytokines (6, 18). In agreement, we observed that the expressions of proinflammatory IL-1, IL-6, and TNF α in both the liver and epididymal fat depots were significantly higher in MKO mice than in *TRAF3^{flox/flox}* mice fed a normal chow diet (Fig. 6A). However, the expressions of IL-1, IL-6, and TNF α in these metabolic tissues were significantly lower in MKO mice than in *TRAF3^{flox/flox}* mice fed a HFD (Fig. 6B). The expression of F4/80 and the number of F4/80-positive cells in the liver were

also lower in HFD-fed MKO mice (Fig. 6, B and C). In epididymal fat depots, the expression of IL-1, IL-6, TNF α , and F4/80 was also significantly lower in HFD-fed MKO mice (Fig. 6B). The number of crown-like structure (a marker of adipose inflammation) was lower in MKO mice (Fig. 6D). FACS analysis revealed that, in epididymal fat depots, macrophage (F4/80⁺ and CD45.2⁺ double positive cells) numbers were significantly lower in MKO mice than in *TRAF3^{flox/flox}* mice fed a HFD (Fig. 6E). Both M1-like (CD45.2⁺ F4/80⁺ CD11c⁺ CD301⁻) and M2-like (CD45.2⁺ F4/80⁺ CD11c⁻ CD301⁺) cell numbers were also lower in obese MKO mice (Fig. 6E). Together, these observations suggest that TRAF3 in myeloid cells has dual immunoproperties (e.g., anti-inflammatory activity in lean mice and proinflammatory activity in obese mice) and switches its activity modes in response to nutritional signals.

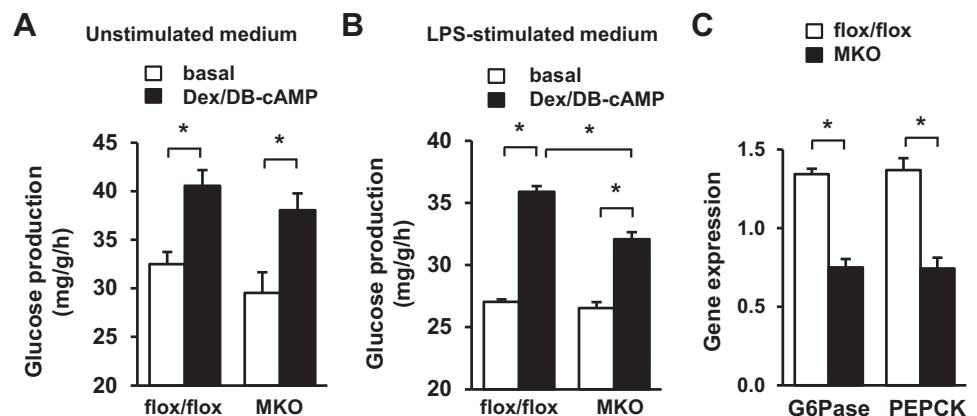
MKO and *TRAF3^{flox/flox}* mice had different inflammatory responses to HFD feeding. In *TRAF3^{flox/flox}* mice, HFD feeding dramatically increased the expressions of IL-1, IL-6, and TNF α in both epididymal fat depots and the liver; however, HFD-stimulated expression of proinflammatory cytokines was either completely blocked or markedly attenuated in MKO mice (Fig. 6F). These observations indicate that TRAF3 in myeloid cells is required for HFD-induced inflammation in metabolic tissues.

DISCUSSION

In this study, we have identified TRAF3 in myeloid cells as a novel metabolic regulator. TRAF3 appears to be necessary for obesity-induced insulin resistance, glucose intolerance, and NAFLD. We have further shown that myeloid TRAF3 may have anti-inflammatory and proinflammatory activities in lean and obese mice, respectively. TRAF3 activity modes appear to be controlled by dietary and/or obesity-associated factors.

We have demonstrated that in *ob/ob* mice, a commonly-used genetic model of obesity, myeloid cell-specific deletion of *TRAF3* dramatically improved hyperglycemia, hyperinsulinemia, glucose intolerance, insulin resistance, and hepatic steatosis. Similarly, myeloid cell-specific deletion of *TRAF3* also attenuated HFD-induced insulin resistance, glucose intolerance, and hepatic steatosis. In agreement with these findings, insulin signaling in the liver, skeletal muscle, and adipose tissue was improved in TRAF3-deficient obese mice. Therefore, myeloid TRAF3 is likely to promote obesity-associated

Fig. 5. TRAF3 cell-autonomously promotes macrophage release of gluconeogenic substances. Conditioned medium was prepared from BMDMs (derived from *TRAF3^{flox/flox}* or MKO mice) treated with or without LPS (20 ng/ml for 4 h). Primary hepatocytes were prepared from wild-type mice (7–10 wk), pretreated the indicated conditioned medium for 4 h, and stimulated without (basal) or with dexamethasone (Dex) and DB-cAMP. *TRAF3^{flox/flox}*, $n = 4$; MKO, $n = 4$. A and B: glucose production in hepatocytes pretreated with conditioned medium collected from unstimulated BMDMs (A) or from LPS-stimulated BMDMs (B). C: expression of *G6Pase* and *PEPCK* was measured by qPCR and normalized to 36B4 expression. Values are presented as means \pm SE. * $P < 0.05$.



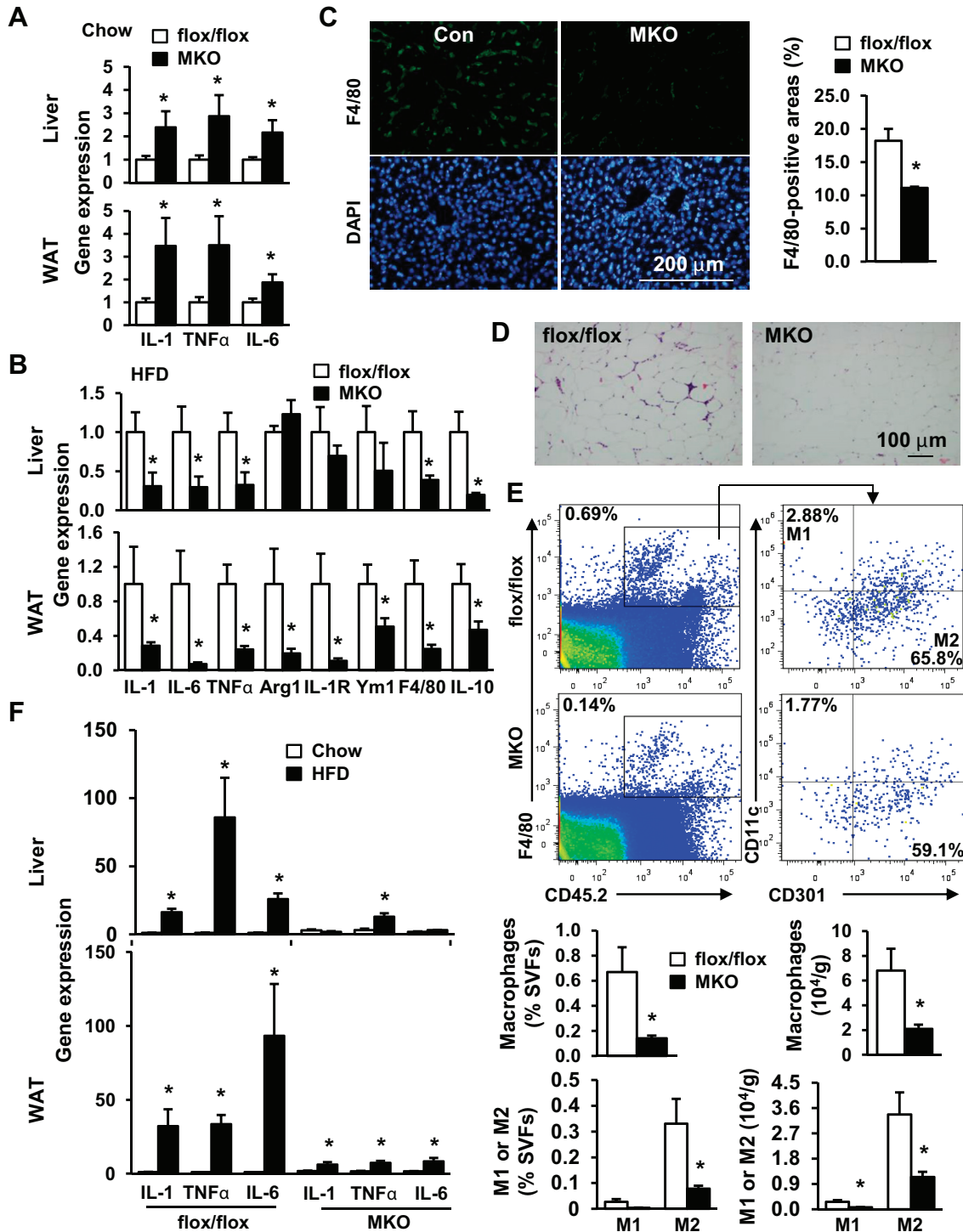


Fig. 6. Obesity-associated factors induce an anti-inflammation to pro-inflammation switch of TRAF3 immunoactivity in myeloid cells. **A**: total mRNA in epididymal fat depots and livers was extracted from male mice fed a normal chow diet at 20 wk of age and used to measure expressions of IL-1, TNF α , and IL-6 by qPCR (normalized to 36B4 expression). *TRAF3^{flox/flox}*, *n* = 11; MKO, *n* = 9. **B–D**: male mice (7–8 wk) were fed a HFD for 10–12 wk. **B**: expression of indicated genes was measured by qPCR in liver and epididymal fat depots. *TRAF3^{flox/flox}*, *n* = 7–11; MKO, *n* = 9–13. **C**: liver sections were prepared from HFD-fed mice and immunostained with anti-F4/80 antibody. F4/80-positive areas were quantified and normalized to total section areas. *TRAF3^{flox/flox}*, *n* = 4; MKO, *n* = 3. **D**: representative H&E staining of visceral adipose tissue sections. **E**: male mice (7–8 wk) were fed a HFD for 8 wk, and stromal vascular fractions (SVFs) were prepared from epididymal fat depots and subjected to FACS analysis. Representative FACS plots of staining for total macrophages (CD45.2⁺F4/80⁺ cells) and M1 (CD11c⁻CD301⁻) and M2 (CD11c⁺CD301⁺) macrophages were presented. Cell frequency (percentage of SVFs, left) and cell content (normalized to tissue weight, right) were calculated. *TRAF3^{flox/flox}*, *n* = 5; MKO, *n* = 5. **F**: male mice (7–8 wk) were fed a chow diet or HFD for 10–12 wk. Gene expression was measured by qPCR and normalized to 36B4 expression. Chow: *TRAF3^{flox/flox}*, *n* = 11; MKO, *n* = 9. HFD: *TRAF3^{flox/flox}*, *n* = 8–11; MKO, *n* = 12–13. Values are presented as means \pm SE. **P* < 0.05.

insulin resistance in metabolic tissues, contributing to hyperglycemia, glucose intolerance, and hepatic steatosis. Deletion of myeloid *TRAF3* also attenuated the hyperglycemic response to glucagon, suggesting that TRAF3 in myeloid cells promotes the ability of counterregulatory hormones to stimulate hepatic glucose production. The molecular mechanism by which myeloid TRAF3 regulates glucagon sensitivity is currently unknown. Insulin is known to suppress glucagon action in the liver; thus, improvement in hepatic insulin action may contribute to the attenuated response to glucagon in MKO mice. Gluconeogenesis rates were lower in primary hepatocytes treated with TRAF3-deficient macrophage-derived conditioned medium than in hepatocytes treated with wild-type macrophage-derived conditioned medium, raising the possibility that myeloid TRAF3 may regulate hepatocyte metabolism in the liver in a paracrine fashion. In activated macrophages, the TRAF3 pathway may increase secretion of progluconeogenesis substances; alternatively, it may suppress the production of antigluconeogenesis substances. Taken together, our data suggest that myeloid TRAF3 may induce an imbalance between insulin and counterregulatory hormone activity in obesity, promoting diabetes progression.

TRAF3 has been well documented to negatively regulate proinflammatory NF- κ B and MAPK pathways and suppress the expression of proinflammatory cytokines in myeloid cells (6, 18, 25). We observed that, in mice fed a normal chow diet, deletion of *TRAF3* in myeloid cells increased the expression of proinflammatory cytokines in both the liver and epididymal fat depots, confirming myeloid TRAF3 as a negative regulator of inflammation in lean mice. Surprisingly, in obese mice, deletion of *TRAF3* in myeloid cells markedly decreased the expression of proinflammatory cytokines in the liver and epididymal fat depots. Liver F4/80-positive macrophage number was lower in HFD-fed MKO mice. The number of adipose macrophages, including both M1-like and M2-like macrophages, was also lower in obese MKO mice. Thus, TRAF3 in myeloid cells appears to have dual inflammatory properties: it suppresses inflammation in lean mice but promotes inflammation in obese mice. In obesity, myeloid TRAF3 may promote metabolic inflammation by increasing both myeloid cell infiltration into metabolic tissues and the expression of proinflammatory cytokines in innate immune cells. The modes of TRAF3 inflammatory activity are likely to be determined by dietary fat content, factors derived from gut microbiota, metabolites, cytokines, metabolic hormones, and/or metabolic states. Therefore, myeloid TRAF3 may be a critical component of the nutrient sensing machinery, which initiates and sustains metabolic inflammation in obesity.

Obesity is associated with activation of cytokine receptors, TLRs, NLRs, and RLRs (2, 5, 9, 14, 23). Cytokines, toxic metabolites, DAMPs, and PAMPs are likely to activate macrophages via these receptors, leading to chronic inflammation in obesity. In myeloid cells, TRAF3 is a common signaling molecule for these ligands and their cognate receptors (7, 25). We observed that deletion of *TRAF3* in myeloid cells largely blocked HFD-induced expression of many proinflammatory cytokines in the liver and adipose tissue, indicating that myeloid TRAF3 is required for diet-induced metabolic inflammation. Inflammation is believed to be a major contributor to insulin resistance and metabolic disease progression in obesity (9, 23). Thus, a diminution in inflammation in obese MKO

mice may be the primary contributor to improved insulin sensitivity and nutrient metabolism in these mice. Thus, myeloid TRAF3 is likely to connect overnutrition to metabolic inflammation, insulin resistance, and metabolic disease. Adipose TRAF3 expression is relatively normal in mice fed a HFD (data not shown). Myeloid TRAF3 may switch its activity modes from anti-inflammation to pro-inflammation in obesity, so therapeutic interventions to reverse this switch is expected to cure insulin resistance, type 2 diabetes, and NAFLD.

In conclusion, we demonstrate that, in mice with either diet-induced or genetic obesity, myeloid cell-specific deletion of *TRAF3* protects against metabolic inflammation, insulin resistance, glucose intolerance, and hepatic steatosis. Our data suggest that myeloid TRAF3 mediates diet-induced metabolic inflammation, thus coupling overnutrition to insulin resistance and NAFLD.

ACKNOWLEDGMENTS

We thank Drs. Lin Jiang, Liang Sheng, Kae Won Cho, and Carey Lumeng for assistance and discussion.

GRANTS

This study was supported by grants DK-091591 and DK-094014 from the National Institutes of Health. This work utilized the cores supported by the Michigan Diabetes Research and Training Center (DK-020572), Michigan Metabolomics and Obesity Center (DK-089503), the University of Michigan's Cancer Center (CA-46592), the University of Michigan Nathan Shock Center (P30 AG-013283), and the University of Michigan Gut Peptide Research Center (DK-34933).

DISCLOSURES

No conflicts of interest, financial or otherwise, are declared by the author(s).

AUTHOR CONTRIBUTIONS

Author contributions: Z.C. and L.R. conception and design of research; Z.C., H.S., C.S., and F.T. performed experiments; Z.C., L.Y., P.Z., Y.L., and L.R. analyzed data; Z.C., L.Y., P.Z., Y.L., and L.R. interpreted results of experiments; Z.C., F.T., and L.R. prepared figures; Z.C., L.Y., F.T., P.Z., Y.L., and L.R. edited and revised manuscript; Z.C., H.S., C.S., L.Y., F.T., P.Z., Y.L., R.B., and L.R. approved final version of manuscript; L.R. drafted manuscript.

REFERENCES

- Bista P, Zeng W, Ryan S, Bailly V, Browning JL, Lukashev ME. TRAF3 controls activation of the canonical and alternative NF κ B by the lymphotoxin beta receptor. *J Biol Chem* 285: 12971–12978, 2010.
- Chawla A, Nguyen KD, Goh YP. Macrophage-mediated inflammation in metabolic disease. *Nat Rev Immunol* 11: 738–749, 2011.
- Chen Z, Sheng L, Shen H, Zhao Y, Wang S, Brink R, Rui L. Hepatic TRAF2 regulates glucose metabolism through enhancing glucagon responses. *Diabetes* 61: 566–573, 2012.
- Cho KW, Zhou Y, Sheng L, Rui L. Lipocalin-13 regulates glucose metabolism by both insulin-dependent and insulin-independent mechanisms. *Mol Cell Biol* 31: 450–457, 2011.
- Glass CK, Olefsky JM. Inflammation and lipid signaling in the etiology of insulin resistance. *Cell Metab* 15: 635–645, 2012.
- Hacker H, Redecke V, Blagoev B, Kratchmarova I, Hsu LC, Wang GG, Kamps MP, Raz E, Wagner H, Hacker G, Mann M, Karin M. Specificity in Toll-like receptor signalling through distinct effector functions of TRAF3 and TRAF6. *Nature* 439: 204–207, 2006.
- Hacker H, Tseng PH, Karin M. Expanding TRAF function: TRAF3 as a tri-faced immune regulator. *Nat Rev Immunol* 11: 457–468, 2011.
- He L, Grammer AC, Wu X, Lipsky PE. TRAF3 forms heterotrimeric complexes with TRAF2 and modulates its ability to mediate NF-(κ)B activation. *J Biol Chem* 279: 55855–55865, 2004.
- Hotamisligil GS. Inflammation and metabolic disorders. *Nature* 444: 860–867, 2006.
- Huang W, Metlakunta A, Dedousis N, Zhang P, Sipula I, Dube JJ, Scott DK, O'Doherty RM. Depletion of liver Kupffer cells prevents the

- development of diet-induced hepatic steatosis and insulin resistance. *Diabetes* 59: 347–357, 2010.
11. **Kosteli A, Soguru E, Haemmerle G, Martin JF, Lei J, Zechner R, Ferrante AW Jr.** Weight loss and lipolysis promote a dynamic immune response in murine adipose tissue. *J Clin Invest* 120: 3466–3479, 2010.
 12. **Liao G, Zhang M, Harhaj EW, Sun SC.** Regulation of the NF-kappaB-inducing kinase by tumor necrosis factor receptor-associated factor 3-induced degradation. *J Biol Chem* 279: 26243–26250, 2004.
 13. **Lumeng CN, Bodzin JL, Saltiel AR.** Obesity induces a phenotypic switch in adipose tissue macrophage polarization. *J Clin Invest* 117: 175–184, 2007.
 14. **Lumeng CN, Saltiel AR.** Inflammatory links between obesity and metabolic disease. *J Clin Invest* 121: 2111–2117, 2011.
 15. **Matsuzawa A, Tseng PH, Vallabhapurapu S, Luo JL, Zhang W, Wang H, Vignali DA, Gallagher E, Karin M.** Essential cytoplasmic translocation of a cytokine receptor-assembled signaling complex. *Science* 321: 663–668, 2008.
 16. **Nieuwdorp M, Giljijamse PW, Pai N, Kaplan LM.** Role of the microbiome in energy regulation and metabolism. *Gastroenterology* 146: 1525–1533, 2014.
 17. **Obstfeld AE, Soguru E, Thearle M, Francisco AM, Gayet C, Ginsberg HN, Ables EV, Ferrante AW Jr.** C-C chemokine receptor 2 (CCR2) regulates the hepatic recruitment of myeloid cells that promote obesity-induced hepatic steatosis. *Diabetes* 59: 916–925, 2010.
 18. **Oganesyan G, Saha SK, Guo B, He JQ, Shahangian A, Zarnegar B, Perry A, Cheng G.** Critical role of TRAF3 in the Toll-like receptor-dependent and -independent antiviral response. *Nature* 439: 208–211, 2006.
 19. **Olefsky JM, Glass CK.** Macrophages, inflammation, and insulin resistance. *Annu Rev Physiol* 72: 219–246, 2010.
 20. **Rui L.** Energy metabolism in the liver. *Comp Physiol* 4: 177–197, 2014.
 21. **Saha SK, Pietras EM, He JQ, Kang JR, Liu SY, Oganesyan G, Shahangian A, Zarnegar B, Shiba TL, Wang Y, Cheng G.** Regulation of antiviral responses by a direct and specific interaction between TRAF3 and Cardif. *EMBO J* 25: 3257–3263, 2006.
 22. **Sheng L, Jiang B, Rui L.** Intracellular lipid content is a key intrinsic determinant for hepatocyte viability and metabolic and inflammatory states in mice. *Am J Physiol Endocrinol Metab* 305: E1115–E1123, 2013.
 23. **Shoelson SE, Goldfine AB.** Getting away from glucose: fanning the flames of obesity-induced inflammation. *Nat Med* 15: 373–374, 2009.
 24. **Sun SC.** The noncanonical NF-kappaB pathway. *Immunol Rev* 246: 125–140, 2012.
 25. **Tseng PH, Matsuzawa A, Zhang W, Mino T, Vignali DA, Karin M.** Different modes of ubiquitination of the adaptor TRAF3 selectively activate the expression of type I interferons and proinflammatory cytokines. *Nat Immunol* 11: 70–75, 2010.
 26. **Watanabe T, Asano N, Fichtner-Feigl S, Gorelick PL, Tsuji Y, Matsumoto Y, Chiba T, Fuss IJ, Kitani A, Strober W.** NOD1 contributes to mouse host defense against *Helicobacter pylori* via induction of type I IFN and activation of the ISGF3 signaling pathway. *J Clin Invest* 120: 1645–1662, 2010.
 27. **Weisberg SP, Hunter D, Huber R, Lemieux J, Slaymaker S, Vaddi K, Charo I, Leibel RL, Ferrante AW Jr.** CCR2 modulates inflammatory and metabolic effects of high-fat feeding. *J Clin Invest* 116: 115–124, 2006.
 28. **Xu Y, Cheng G, Baltimore D.** Targeted disruption of TRAF3 leads to postnatal lethality and defective T-dependent immune responses. *Immunity* 5: 407–415, 1996.
 29. **Yuan M, Konstantopoulos N, Lee J, Hansen L, Li ZW, Karin M, Shoelson SE.** Reversal of obesity- and diet-induced insulin resistance with salicylates or targeted disruption of Ikkbeta. *Science* 293: 1673–1677, 2001.
 30. **Zarnegar B, Yamazaki S, He JQ, Cheng G.** Control of canonical NF-kappaB activation through the NIK-IKK complex pathway. *Proc Natl Acad Sci USA* 105: 3503–3508, 2008.
 31. **Zhu S, Pan W, Shi P, Gao H, Zhao F, Song X, Liu Y, Zhao L, Li X, Shi Y, Qian Y.** Modulation of experimental autoimmune encephalomyelitis through TRAF3-mediated suppression of interleukin 17 receptor signaling. *J Exp Med* 207: 2647–2662, 2010.

